Journal of Solid State Chemistry **154**, 93–100 (2000)
doi:10.1006/jssc.2000.8817, available online at http://www.idealibrary.com on IDEAL®

Modulated Photoconductivity of High-Purity and Carbon-Doped β-Rhombohedral Boron

H. Werheit, M. Schmidt, and R. Schmechel[1]

Solid State Physics Laboratory, Gerhard-Mercator University, D-47048 Duisburg, Germany

and

T. Lundström

The Ångström Laboratory, Uppsala University, Box 538, S-75121 Uppsala, Sweden

Received September 9, 1999; in revised form January 21, 2000; accepted January 30, 2000

Frequency-modulated photoconductivity spectra of high-purity and up to 1.1 at.% carbon-doped β-rhombohedral boron were measured between about 96 and 380 K to get information on electronic transport with small relaxation times. At $T < 190$ K steps in the photoconductivity spectra are correlated with the occupied well-known electron traps. Between about 250 and 350 K the low-energy photoconductivity shows peaks at about 0.23 and 0.46 eV, which can be attributed to carbon donor states in the band gap. For $T > 170$ K the interband recombination is fast enough to become appreciable in the dark phase of the modulation, and the interband photoconductivity becomes prevailing. The interband transition energies known from absorption measurements are confirmed. The thermal activation energy of the electron mobility is about 14 meV, probably due to a shallow level off the conduction band. © 2000 Academic Press

INTRODUCTION

Aside from boron carbide, β-rhombohedral boron is the best-investigated and best-understood icosahedral boron-rich solid. An energy band scheme with a gap of about 1.5 eV and numerous gap states (see (1) 1 and references therein) makes it possible to describe the different electronic properties largely consistently. The band gap is essentially determined by the Jahn–Teller splitting of the orbitals of the icosahedron (2) The electron deficiency of the idealized structure (3) is compensated by structural defects, in particular by vacancies generating acceptor states in the band gap (4). Carbon atoms substitute for B atoms in polar sites of the icosahedra (5, 6), They are assumed to generate deep-lying donor states close to defect states in the gap. For the actual band scheme, including the electronic levels obtained in the present paper and those presented in (15), see below (Fig. 12).

Photoeffects like photoabsorption, photoconductivity, and photo-ESR, have played an essential role in elucidating the electronic properties of this semiconductor (see (1) and references therein). The disadvantage of steady-state photoeffects is that processes with large and small relaxation times cannot be distinguished. In particular in β-rhombohedral boron, where long-lasting relaxation processes are dominating by far, information on processes with small relaxation times is largely missing. This is accessible for example by modulated photoconductivity measurements, whose results are presented in this paper.

SAMPLE MATERIAL

The following samples have been investigated:

1. Single-crystal β-rhombohedral boron (Wacker Chemistry, Munich), crystallographic orientation unknown, purity 99.9999%, apart from carbon (typically 30–120 ppm). The sample is first mechanically polished on a rotating disk (Struers) with diamond spray, gradually reduced to grain size (final 1 μm), and then chemically etched (weight relation of the solution, H_2O:$K_3[Fe(CN)_6]$: KOH = 70:22:8 (7)).
2. Single-crystal β-rhombohedral boron (Wacker Chemistry, Munich), like sample 1, however not chemically etched.
3. C-doped polycrystalline β-rhombohedral boron (C, 0.11 at.%). The sample is prepared from boron (Wacker, Munich, 99.99% purity) and carbon (Cerac, Milwaukee, 99.95% purity) by arc melting and subsequent annealing for

[1] Present address: Darmstadt University of Technology, Material Science, Department of Electronic Materials, D 64287 Darmstadt, Germany.

0022-4596/00 $35.00
Copyright © 2000 by Academic Press
All rights of reproduction in any form reserved.

48 h at 1300°C in a carbon-free furnace (Ta element) filled with 0.5×10^5 Pa argon.

4. C-doped polycrystalline β-rhombohedral boron (C, 0.43 at.%). Preparation is like that of sample 3.
5. C-doped polycrystalline β-rhombohedral boron (C, 1.1 at.%). Preparation is like that of sample 3.
6. Single-crystal β-rhombohedral boron (Research Center for Crystals, Warsaw), orientation unknown. The typical analysis of a probably comparable material (in ppm) is as follows: C, 3250; Na, 18; K, 74; Mg, 6; Ca, 8.5; Al, 3.5; Si, 18; N, 53; P, 2; O, 260; S, 4; Cl, 3.5; Cu, 1.5; Ti, 14; Nb, 1.5; Cr, 13; W, 14; Fe, 7; and Ni, 5. (For an estimation of the C content (1.65(5) at.%) from photoconductivity results, see below.) Preparation is like that of sample 1.

Ohmic probes were attached with Pt wires of 0.1 mm diameter fixed to the samples by a capacitor discharge. Those contacts are formed by a low-melting B–Pt eutectic.

The influence of the surface properties on the interband photoconductivity, which depends on the penetration depth of the exciting light, is demonstrated for one sample, whose surface for the first measurement was mechanically polished only and afterward for the second measurement chemically etched (Fig. 1). The influence of the surface properties depends considerably on temperature.

EXPERIMENTAL

Six deep electron traps with ionization energies of multiples of 190 meV (1) determine the relaxation of the dc photoconductivity in β-rhombohedral boron. The relaxation times are therefore very long (results attributed to the first four traps, ~ 7, ~ 80, ~ 700, and $\sim 1.5 \times 10^4$ s (8, 9)). Accordingly, the 12-Hz modulated photoconductivity yields the small derivative in the 0.083-s time interval and is nearly exclusively determined by processes with very short relaxation times.

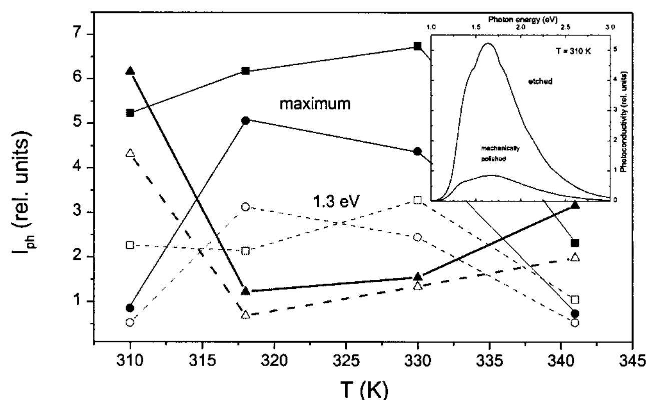

FIG. 1. Interband photoconductivity spectrum of high-purity β-rhombohedral boron samples. Maximum values (solid symbols) and values at 1.3 eV (open symbols) vs temperature: Squares, only mechanically polished; circles, additionally chemically etched; triangles, quotient I_{ph}(etched)/I_{ph}(mech. polished). Inset: spectra at 310 K.

To obtain well-defined starting conditions, before each measurement the samples were heated in darkness to 380 K and kept at this temperature for 1 h, where a rather quick relaxation to the thermal equilibrium with largely emptied traps is expected. Then the samples were quickly cooled in complete darkness within about 10 min. to the temperature of measurement. Accordingly the starting condition is not the thermal equilibrium at this temperature but largely that frozen-in from 380 K. However, this does not mean that electrons thermally excited into the traps are frozen in, because in this case the photoconductivity spectra of trapped electrons should be found at low temperatures without additional optical excitation, and this is not the case (see below). After new results of dc photoconductivity (10), at 380 K a structural relaxation seems to take place, which is accompanied by a monotonically increasing electrical conductivity and is responsible for structural effects like hysteresis of the thermal expansion and maxima of internal friction (see (1, 16) and references therein).

Two photoconductivity spectra were measured at each temperature. After the temperature of measurement was reached, the sample was kept in darkness for about 1 h to allow the development of a quasi-thermal equilibrium. Then the first spectrum was measured with only weak spectral light reaching the sample. A second spectrum was obtained, after the sample was excited for 1 h by a xenon arc-lamp, whose radiation of the range $\lambda \gtrsim 1$ μm was cut by an optical edge filter.

To detect small signals, the periodically illuminated sample was in a bolometer-type arrangement with an unilluminated sample of the same kind in series. Hence both branches of this bridge have the same temperature-dependent resistances, and an electrical readjustment of the setup at different temperatures was avoided. The resulting 12-Hz ac signal was measured with lock-in technique. Nevertheless, the detection of small signals required long integration times. Therefore the complete program of measurement was controlled by suitably composed computer software.

RESULTS

Gap-State-Determined Photoconductivity

At photon energies below the interband transitions, depending on temperature two different kinds of spectra were obtained for high-purity boron. At temperatures $T \lesssim 205$ K, where the interband recombination is too slow to be detectable within the 12-Hz period, there is no photoconductivity without, but a step-like photoconductivity after preexcitation with the xenon arc lamp (Fig. 2). Obviously, this photoconductivity is due to the excitation of trapped electrons. Their excitation takes place homogeneously within the bulk,

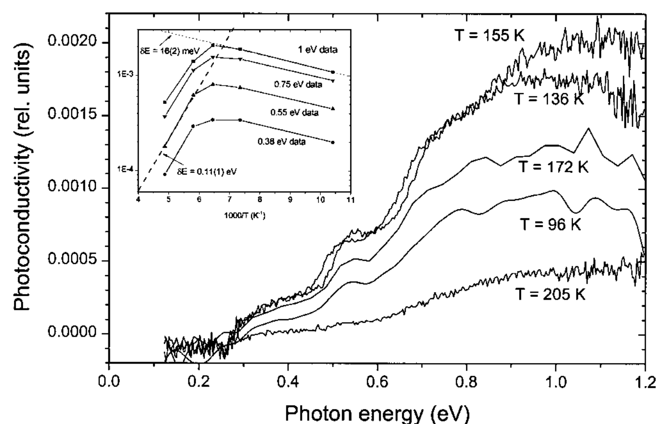

FIG. 2. Gap-state related photoconductivity of high-purity β-rhombohedral boron (etched sample) at temperatures $\lesssim 205$ K vs photon energy. Inset: temperature-dependence of the photoconductivity. Log photoconductivity vs reciprocal temperature for the different steps.

and therefore the level of the step is largely independent of energy, and there is no energy-dependent surface recombination expected like that of interband photoconductivity caused by the penetration depth of the exciting radiation decreasing with increasing photon energy. The measured ac signal in this temperature range is due to the excitation of electrons in the bright period and retrapping in the dark period of the modulation.

Because of the largely homogeneous excitation in bulk the energy dependence of the photoconductivity is proportional to the combined density of states. Therefore the ionization energies can be determined as in the case of optical absorption, where the theory for deep levels to band transitions (11) was successfully applied (12, 16, 17). The results are listed in Table 1 and compared with the energies determined from the absorption spectra. For boron with the highest C content (1.1 at.%) the photoconductivity in this spectral range was below the detection limit.

The level of the steps is thermally activated with $\delta E = 16(2)$ meV, which is the same for all steps. Therefore we attribute this activation energy to the free electron mobility in the conduction band, possibly caused by a hitherto unknown shallow level below the conduction band edge. Absorption bands in the FIR spectrum at 11.9, 17.7, 20.1, and 25.0 meV (13, 14) can probably be attributed to such a shallow level.

Toward higher temperatures this step-like photoconductivity, essentially determined by the occupation densities of the electron traps, decreases according to a thermal activation energy of 0.11(1) eV, independent of the specific step. Following the photoluminescence results, this can be explained by a thermally activated cascade-like recombination of trapped electrons into the valence band (15). In this recombination path electrons captured in trap n are thermally excited into the level of the unoccupied trap $n+1$, whose energy subsequently decreases by relaxation into the equilibrium of the occupied state $n+1$ (see Fig. 12). The present result seems to confirm the conclusion in (15) that the excitation energy of 0.12 eV is independent of n.

In the temperature range $250 < T < 350$ K the gap-state-related photoconductivity exhibits a relatively strong peak with maximum at 0.26(1) eV and a weaker peak with maximum at 0.52(1) eV (Fig. 3). The maximum of the strong peak increases with temperature according to a thermal excitation energy of 0.23(2) eV and decreases at higher temperatures according to an activation energy of 0.66(2) eV. The intensity of these peaks is partly quenched (thermal excitation energies change to 0.29 eV) by the excitation with the xenon lamp similar to that of the interband photoconductivity. This suggests attributing these peaks to gap states related to the valence band. The excitation of free holes from the defect level (~ 0.19 eV above the valence band edge) can be excluded, because this transition is forbidden by selection rules (15, 16). From several investigations it was concluded that C atoms generate a donor level close to this defect level (17), and Fig. 4 shows that the normalized intensity of the greater peak increases with increasing C content. Regarding the slope in Fig. 4, it must be considered that this normalization is questionable in so far

TABLE 1
Ionization Energies of Electron Traps in β-Rhombohedral Boron

	Ionization energies (eV)					
	Trap 1	Trap 2	Trap 3	Trap 4	Trap 5	Trap 6
Photoconductivity (this work)						
High-purity β-rh. B	0.20(2)	0.40(2)	0.59(2)	0.80(3)	0.99(4)	
0.11 at.% C	0.21(3)	0.37(5)	0.58(2)			
0.43 at.% C		0.38(4)	0.56(5)			
Optical absorption (12, 16, 17)						
B_{12} icosahedra in β-rh. B	0.17(2)	0.37(2)	0.58(2)	0.76(2)	0.95(3)	1.15(4)
$B_{11}C$ icosahedra in β-rh. B	0.21(2)	0.41(2)	0.60(2)	0.82(2)	1.02(3)	1.21(3)

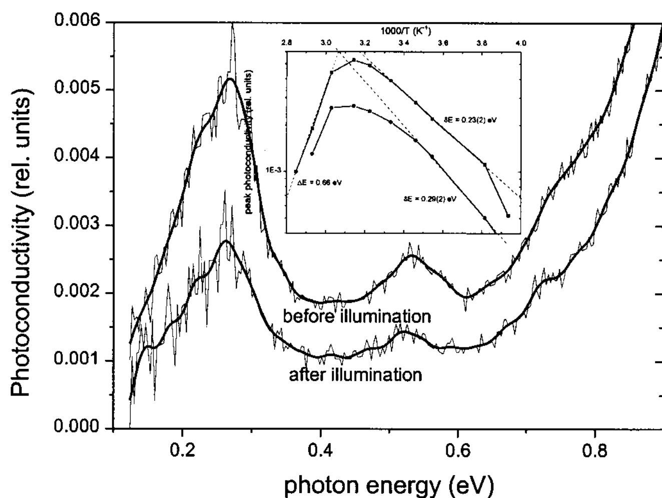

FIG. 3. Gap-state related photoconductivity of high-purity β-rhombohedral boron (etched sample) in the temperature range $250 \lesssim T \lesssim 350$ K. Measured (weak lines) and smoothed data (strong lines) vs photon energy, before and after optical excitation with a xenon arc lamp. Inset: temperature dependence of the strong peak.

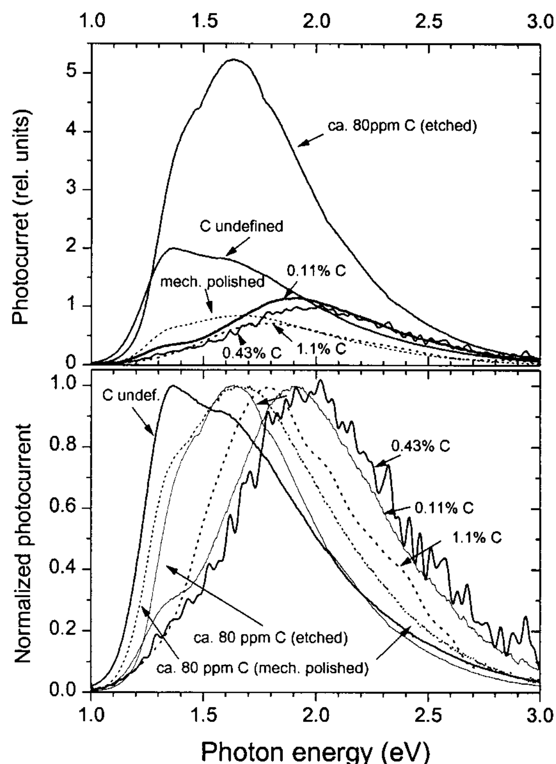

FIG. 5. Interband photoconductivity spectra for samples with different carbon contents and different surface preparation (the C-doped samples were only mechanically polished): (a) as measured (samples had approximately the same size) and (b) normalized to the curve maxima.

that the interband recombination velocity increases with increasing C content and therefore the lifetime of free carriers, which is one specific parameter of the photoconductivity, decreases. Hence the interband photoconductivity could not only depend on the sample preparation but also on its C content.

For transitions from the valence band into the C states in the gap no selection rules are expected. Hence we attribute this level with $\delta E = 0.26$ eV above the valence band to the donor level of carbon in β-rhombohedral boron. The photoconductivity peak at 0.52 eV could be due to an excited level of the C donor.

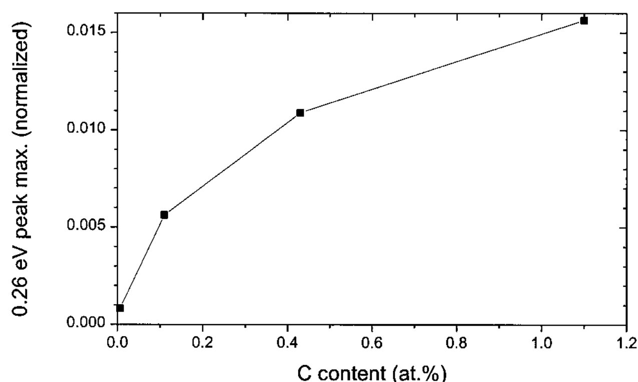

FIG. 4. Normalized intensity of the 0.26-eV peak maximum in Fig. 3 vs carbon content. To eliminate the influence of different sample preparation (etched high-purity boron, only mechanically polished C-doped boron) the data are normalized in relation to the interband photoconductivity maximum.

Interband Photoconductivity

The 12-Hz-modulated interband photoconductivity is measurable between about 180 and 400 K with a maximum at about 330 K. The interband photoconductivity spectra of different samples measured at room temperature are displayed in Fig. 5.

From the derivatives of the measured photoconductivity spectra the critical points of electronic transitions were determined. Figure 6 shows that most of them satisfactorily agree with the transitions determined by optical absorption (16); recently the low-energy transitions were attributed to transitions from defect states in the gap into the conduction band (15, 18): Additionally, for C-doped samples transitions at energies between about 1.05 and 1.13 eV occur, indicating levels at about 0.5 eV above the valence band edge in rough agreement with the energy position of one of the photoconductivity peaks in Fig. 3 attributed above to carbon.

The temperature dependence of the maximum of the modulated interband photoconductivity is displayed in Fig. 7. Some relations to the conditions in β-rhombohedral boron are found in the theory of a two-trap model of p-type amorphous semiconductors by Simmons and Taylor (19);

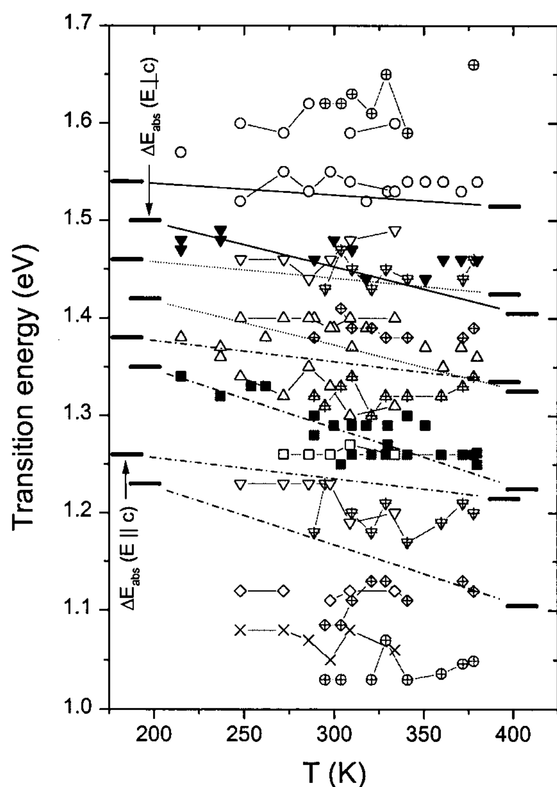

FIG. 6. Excitation energies of high-purity (etched sample) and C-doped β-rhombohedral boron (mechanically polished samples) obtained from the difference spectra (unexcited minus optically excited) compared with the interband transition energies determined from optical absorption. Closed symbols, high-purity B; crossed symbols, carbon-doped B (0.11 at.% C); open symbols, carbon-doped B (1.65 at.% C estimated, see below). Bars connected by solid lines, interband transitions with phonon emission; bars connected with dotted lines, interband transitons with phonon absorption; bars connected with dash–dotted lines, transitions from defect states into the conduction band [(20) luminescence and references therein].

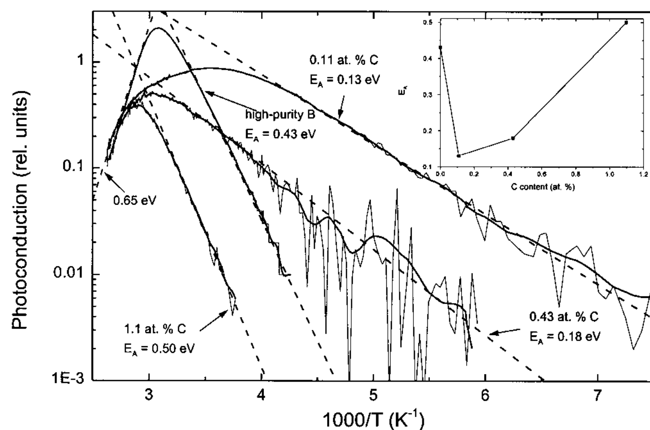

FIG. 7. Temperature dependence of the maximum interband photoconductivity of high-purity (etched sample) and C-doped β-rhombohedral boron (mechanically polished samples). Thin lines, as measured; bold lines, smoothed data. Broken lines, fits to determine the thermal activation energies. Inset: low-temperature activation energies plotted vs carbon content.

indeed it must be accepted that the theory deals with steady-state photoconductivity. According to this theory two ranges are to be distinguished:

(i) The high temperature range is characterized by a "low excitation level," where the concentration of optically excited carriers is small compared with those thermally excited. In this range the photoconductivity decreases with increasing temperature. The activation energy theoretically expected is half the difference between the conduction band edge and the uppermost occupied valence band state, that is, in the case of boron the difference between the Fermi level and the hole trapping level at about ~ 0.19 eV above the valence band edge (4). Accordingly, it is not surprising that the thermal activation energy of 0.65 eV is the same for high-purity and C-doped boron and agrees with the activation energy of the intrinsic electrical conductivity (see (1) and references therein). However, for the integral interband photoconductivity spectra the result is different (Fig. 8); there is a strong nonmonotonic dependence of the activation energy on the carbon content. The difference of the conditions of measurement is as follows: Because of the long time of measurement at each temperature, a kind of thermal equilibrium could have developed. The result makes sense as well, if one assumes that the Fermi level in the gap is shifted toward the valence band when additional occupied states are introduced by carbon close to the valence band. However, the qualitative difference of both results shows that the antecedent has significant influence on the photoconductivity.

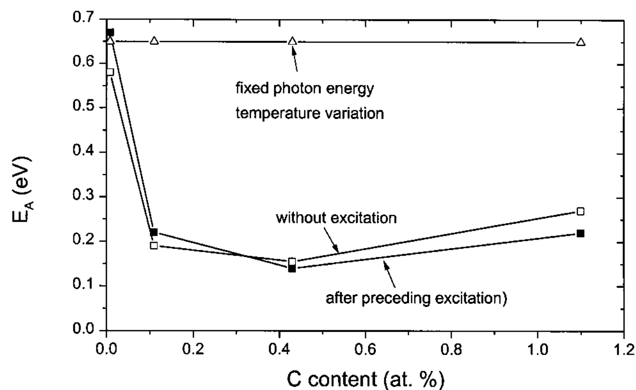

FIG. 8. Thermal activation energy of decreasing of the interband photoconductivity with increasing temperature. Triangles, obtained from Fig. 7 (temperature-dependent variation at fixed photon energies); squares, obtained from the integral interband photoconductivity spectra measured at fixed temperatures, after thermal equilibrium has largely been developed.

(ii) The "moderate-level" range is at lower temperatures, where for the two-trap model $E_A = (E_{trap} - E_V)/2$ is expected. The results for pure and C-doped boron are displayed in the inset of Fig. 7. For the integral interband photoconductivity spectra plotted accordingly the results are the same within the accuracy of measurement. In this temperature range the simple two-trap model is obviously not sufficient for boron, in particular not for the modulated photoconductivity comprehending fast processes only. For boron with the highest C content (1.1 at.%) the activation energy corresponds to the level at about 0.5 eV above the valence band edge, which was attributed above to carbon. If the electron transfer from the C atoms to the boron framework is sufficient to fill up the states closer to the valence band edge, the generation of free holes with small relaxation times would require this activation energy. For smaller C contents this generation of free holes will occur by electron transitions into the states closer to the valence band in rough agreement with the determined activation energies. However, for high-purity boron there is no perceptible correlation between the activation energy and known gap states.

Irrespective of whether the samples are pure or carbon-doped, in the interband photoconductivity spectra discussed till now the transition at about 1.3 eV, which is attributed to the electrons excited from the defect states into the conduction band, was distinctly weaker than the transitions from the valence into the conduction band, in accordance with the relation of the densities of states. However, the spectrum of the Warsaw single crystal (sample 6) exhibits in this range a peak distinctly stronger than the interband photoconductivity peak (Fig. 9). Unfortunately, there is no chemical analysis for this individual sample available. Therefore we can only speculate that a very high carbon content of this sample is the reason. Indeed, this speculation is supported by the activation energies of the integral interband photoconductivity. By a rough linear extrapolation of the data in the inset of Fig. 7 the low-temperature activation energy of 0.61 eV leads to an estimated C content of about 1.6 at.%, and the corresponding extrapolation of the high-temperature activation energies in Fig. 8 to about 1.7 at.% C. Then, in consequence of the high additional electron concentration of carbon donors, an accordingly high concentration of defects states (acceptors) is expected to be generated for compensation. (see (4)), and these defect levels are at energies of 1.23 to 1.37 eV below the conduction band (4), in agreement with the photoconductivity spectra of this material.

In Fig. 10 as typical examples the spectra for 330 K and as untypical examples the spectra for 318 K obtained before and after illumination with the xenon arc lamp and their differences are displayed. In the typical difference spectra the peaks attributed to the transition from gap states and that from the valence band respectively are clearly seen. The maximum values plotted in Fig. 11 vs reciprocal temperature are thermally activated in the increasing and in the decreasing range respectively. The activation energy for the increase of the main peak of the difference spectra is equal to that of the integral photoconductivity. The activation energy of the small peak confirms its attribution to gap states, because the fast transport process measured with the modulation method requires thermal activation of free holes from the valence band in that energetical distance. The activation energy determined from the decrease of the photoconductivity toward high temperatures in Fig. 11 is nearly equal to the band gap.

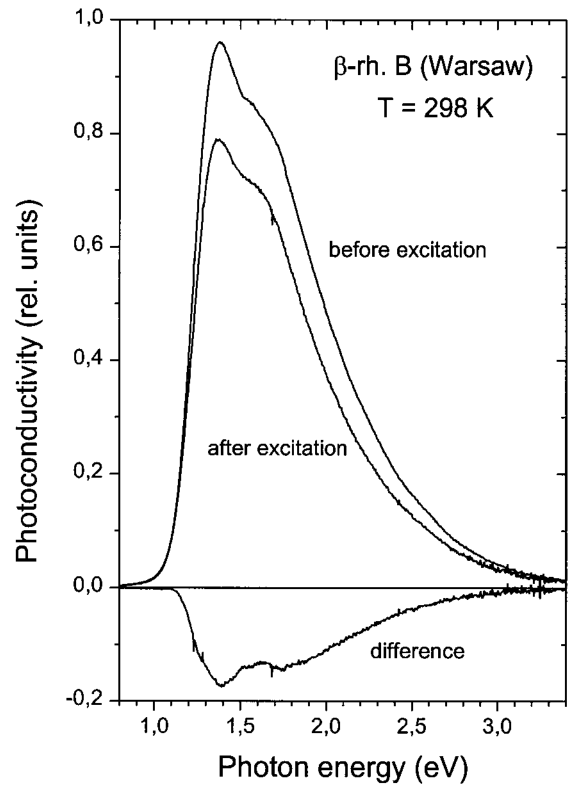

FIG. 9. Photoconductivity spectra of sample 6 (single crystal from Warsaw, etched) at 298 K before and after optical excitation with the xenon arc lamp, and the difference spectrum.

The difference spectrum at 318 K is untypical because it is the only one that does not show any trace of the transition at 1.3 eV. Therefore the corresponding point in Fig. 11 does not fit to the others. The reason is the antecedent of the sample for that measurement, which is different from the usual heating to 380 K for 1 h and quickly cooling (~10 min.) to the temperature of measurement. This way the conditions of thermal equilibrium at 380 K were frozen in. For the spectrum at 318 K the sample was heated to 380 K as usual, but the cooling procedure lasted for about

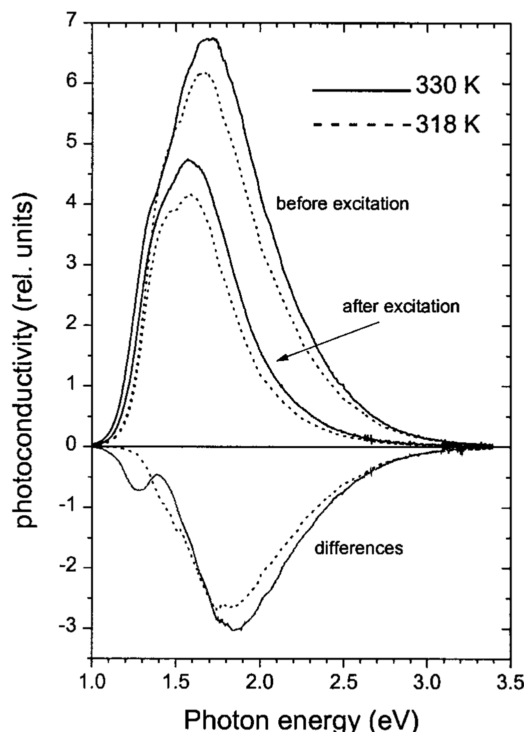

FIG. 10. Typical interband photoconductivity spectra of high-purity etched β-rhombohedral boron (before and after optical excitation) and their difference (example at $T = 330$ K). The conditions for obtaining this spectrum, in particular the antecedent, are the same as those for the spectra presented in Fig. 9. The untypical spectrum (318 K) is due to a different antecedent (see text).

12 h, and therefore thermal equilibrium at the temperature of measurement can largely be assumed. This again demonstrates the high sensibility of the electronic properties of β-rhombohedral boron on the antecedent.

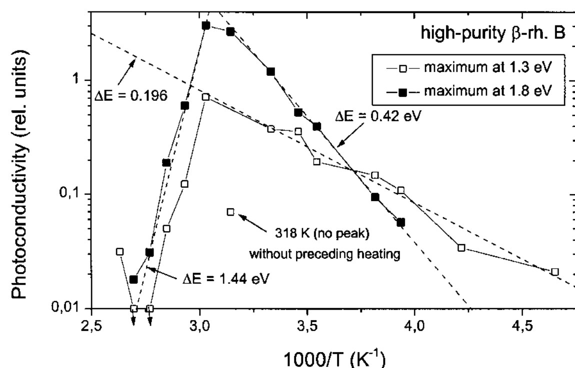

FIG. 11. Intensity of the interband photoconductivity maxima of high-purity β-rhombohedral boron (etched) vs reciprocal temperature. Dashed lines, fits to determine the thermal activation energies.

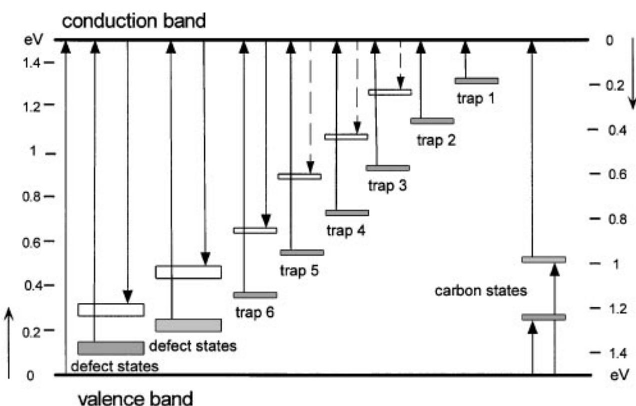

FIG. 12. Actual band scheme of β-rhombohedral boron based on a band gap of approximately 1.5 eV. The energy positions of the occupied levels are marked by filled rectangles, those of the corresponding unoccupied states (see (15)) by hollow rectangles. Experimentally determined transitions by optical absorption, photoabsorption (see (1)), or photoconductivity (this paper) are shown by solid arrows, assumed, but not yet experimentally proved transitions, by broken arrows.

CONCLUSION

The modulated photoconductivity confirms the existence and energy position of the electron traps in the band gap of β-rhombohedral boron, and it directly proves that at low temperatures the excitation of trapped electrons into the conduction band leads to a measurable electronic transport by free electrons. The mobility of the electrons is thermally activated at about 14 meV. At low temperatures the retrapping rate exceeds the recombination rate considerably. The results confirm the cascade-like nonradiating recombination of trapped electrons (15). The energy position of the carbon donors close to the defect states in the band gap was quantitatively determined. The actual band scheme, displayed in Fig. 12, is based on previous results of optical and transport investigations (see (1)) and considers the results in the present paper and the positions of the unoccupied levels derived from the photoluminescence spectra (15, 20).

The strong dependence of the photoconductivity on the antecedent is obvious. The effects of moderate temperatures (400–600 K) on structural and electronic properties were discussed in (16). In connection with the results obtained in (4, 15) it is assumed that at those temperatures and probably already at somewhat lower temperatures a diffusion of interstitial B atoms into energetically more favorable sites takes place (10). This could, for example, influence the density of gap states and could be the reason for the vanishing of the photoconductivity peak at 1.3 eV.

ACKNOWLEDGMENTS

The authors are grateful to Wacker Chemistry, Munich, for providing the boron for samples no. 1–5, Mrs. A.-S. Ullström, Uppsala University, for

assistance in synthesis of the carbon-doped boron; and Dr. A. J. Nadolny, Physical Institute of the Polish Academy of Sciences, Warsaw, for providing sample no. 6.

REFERENCES

1. H. Werheit and R. Schmechel, *in* "Landolt-Börnstein, Numerical data and functional relationships in Science and Technology, Group III" (O. Madelung, Ed.), Vol. 41C, p. 3. Springer-Verlag, Berlin, 1998.
2. M. Fujimori and K. Kimura, *J. Solid State Chem.* **133,** 178 (1997).
3. D. W. Bullett, *J. Phys. C: Solid State* **15,** 415 (1982).
4. R. Schmechel and H. Werheit, *J. Phys.: Condens. Matter* **11,** 6803 (1999).
5. H. Werheit, U. Kuhlmann, and T. Lundström, *J. Alloys Compd.* **204,** 197 (1994).
6. H. Werheit, U. Kuhlmann, and T. Lundström, *in* "Proceedings 11th International Symposium on Boron, Borides and Related Compounds, Tsukuba, Japan, August 22–26, 1993" (R. Uno and I. Higashi, Eds.), Japan. *J. Appl. Phys. Series*, Vol. 10, p. 5.
7. H. Binnenbruck, A. Hausen, P. Runow, and H. Werheit, *Z. Naturforsch. A* **25,** 1431 (1970).
8. H. Werheit, F. Kristen, and R. Franz, *phys. Stat. Sol. B* **172,** 405 (1992).
9. H. Werheit and F. Kummer, *J. Phys.: Condens. Matter* **7,** 7851 (1995).
10. H. Werheit and B. Wehmöller, to be published.
11. G. Lucovsky, *Solid State Commun.* **3,** 299 (1965).
12. H. Werheit and U. Kuhlmann, *Solid State Commun.* **88,** 21 (1993).
13. H. Binnenbruck and H. Werheit, *Z. Naturforsch. A* **34,** 787 (1979).
14. U. Kuhlmann, Thesis, Gerhard-Mercator University of Duisburg, Duisburg, Germany, 1994.
15. R. Schmechel and H. Werheit, *J. Solid State Chem.* **154,** 000 (2000).
16. H. Werheit, M. Laux, and U. Kuhlmann, *Phys. Stat. Sol. B* **176,** 415 (1993).
17. H. Werheit, U. Kuhlmann, M. Laux, and T. Lundström, *Phys. Stat. Sol. B* **179,** 489 (1993).
18. R. Schmechel, Thesis, Gerhard-Mercator University of Duisburg, Duisburg, Germany, 1998.
19. J. G. Simmons and G. W. Taylor, *J. Phys. C: Solid State Phys.* **7,** 3051 (1974).
20. R. Schmechel and H. Werheit, *J. Solid State Chem.* **154,** 68 (2000).